Applied Surface Science 255 (2009) 3933–3939

Contents lists available at ScienceDirect

Applied Surface Science

journal homepage: www.elsevier.com/locate/apsusc

Characteristics and heat treatment of cold-sprayed Al–Sn binary alloy coatings

Xian-Jin Ning [a], Jin-Hong Kim [a], Hyung-Jun Kim [a,*], Changhee Lee [b]

[a] Welding Research Center, Research Institute of Industrial Science & Technology, Pohang 790-600, Republic of Korea
[b] Kinetic Spray Coating Laboratory, Division of Materials Science and Engineering, Hanyang University, Seoul 133-791, Republic of Korea

ARTICLE INFO

Article history:
Received 22 May 2008
Received in revised form 24 September 2008
Accepted 10 October 2008
Available online 31 October 2008

Keywords:
Cold gas dynamic spray
Bearing materials
Al–Sn binary coating
Heat treatment
Bond strength

ABSTRACT

In this study, Al–Sn binary alloy coatings were prepared with Al–5 wt.% Sn (Al–5Sn) and Al–10 wt.% Sn (Al–10Sn) gas atomized powders by low pressure and high pressure cold spray process. The microstructure and microhardness of the coatings were characterized. To understand the coarsening of tin in the coating, the as-sprayed coatings were annealed at 150, 200, 250 and 300 °C for 1 h, respectively. The effect of annealing on microstructure and the bond strength of the coatings were investigated. The results show that Al–5Sn coating can be deposited by high pressure cold spray with nitrogen while Al–10Sn can only be deposited by low pressure cold spray with helium gas. Both Al–5Sn and Al–10Sn coatings present dense structures. The fraction of Sn in as-sprayed coatings is consistent with that in feed stock powders. The coarsening and/or migration of Sn phase in the coatings were observed when the annealing temperature exceeds 200 °C. Furthermore, the microhardness of the coatings decreased significantly at the annealing temperature of 250 °C. EDXA analysis shows that the heat treatment has no significant effect on fraction of Sn phase in Al–5Sn coatings. Bonding strength of as-sprayed Al–10Sn coating is slightly higher than that of Al–5Sn coating. Annealing at 200 °C can increase the bonding strength of Al–5Sn coatings.

1. Introduction

In cold gas dynamic spray (CGDS, or simply cold spray), the spray particles (ductile metal or composite powder with typical size less than 50 μm) can be accelerated to a velocity of about 300–1200 m/s by supersonic gas jet generated by a de Laval type nozzle [1,2]. As the particle velocity exceeds a so called critical velocity, the interface bonding between the particle and substrate will occur with localized deformation under high strain rate and adiabatic shear instability [3–7]. The fact that the particles experienced a temperature well below the melting point of the spray materials makes it feasible to deposit metal coatings such as Al, Cu, Ni, etc., or metal–metal composite coatings such as Cu–Co, Cu–W, Al–Ni with low oxygen content and low porosity. These peculiarities of cold spraying attracted more and more interests in recent years [8,9].

Al–Sn based alloys are widely used as sliding bearing materials in automobile and shipbuilding industry [10,11]. In these alloy systems, tin is a necessary soft phase in the aluminum matrix. Due to its low modulus, low strength and the excellent anti-welding characteristics with iron, tin phase in Al–Sn bearing materials can provide suitable friction properties and shear surface during sliding [10]. The conventional manufacturing for the bearings involves casting and thermo-mechanical processing to bond the Al–Sn layers onto steel back. In this process, a series of intermediate heat treatment and careful control of parameters are necessary for the control of microstructure and property. To avoid the complexity and cost of the conventional process, HVOF spray process has been introduced by McCartney to prepare Al–Sn–Si bearing alloy coatings. Post heat treatment of the HVOF-sprayed coating at 300 °C proved the coarsening of tin and precipitate of Si in the coating [12,13]. Based on the feasibility of preparing oxygen sensitive metal coatings, cold spray was also introduced to deposit Al–Sn binary alloy coatings recently [14].

In the prior study [14], dense coatings of Al–10Sn and Al–20Sn binary alloy were prepared by low pressure cold spray process with helium gas. However, it is quite difficult to deposit the Al–10Sn coating by both low pressure and high pressure cold spray system when nitrogen was used as the propellant gas. Therefore, in this study the Al–10Sn coating was prepared by low pressure cold spray with helium while Al–5Sn by high pressure cold spray with nitrogen gas. The microstructure and microhardness of the as-sprayed coatings were characterized. To understand and control the coarsening of Sn phase in the coating during heat treatment, the coatings were annealed at different temperature. The effect of heat treatment on microstructure, content of Sn and properties

* Corresponding author. Tel.: +82 54 279 5444; fax: +82 54 279 6879.
E-mail address: khyungj@rist.re.kr (H.-J. Kim).

0169-4332/$ – see front matter © 2008 Elsevier B.V. All rights reserved.
doi:10.1016/j.apsusc.2008.10.074

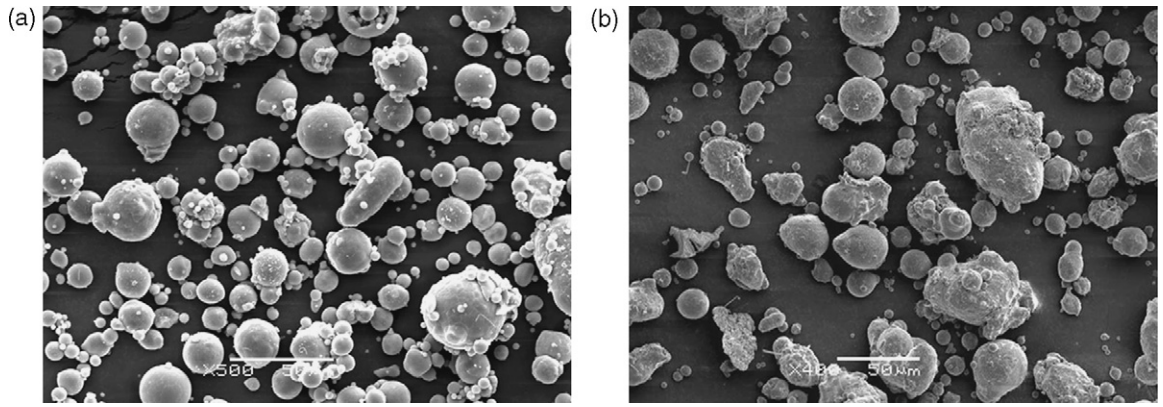

Fig. 1. SEM morphology of Al–Sn feed stock powders; (a) Al–5Sn and (b) Al–10Sn.

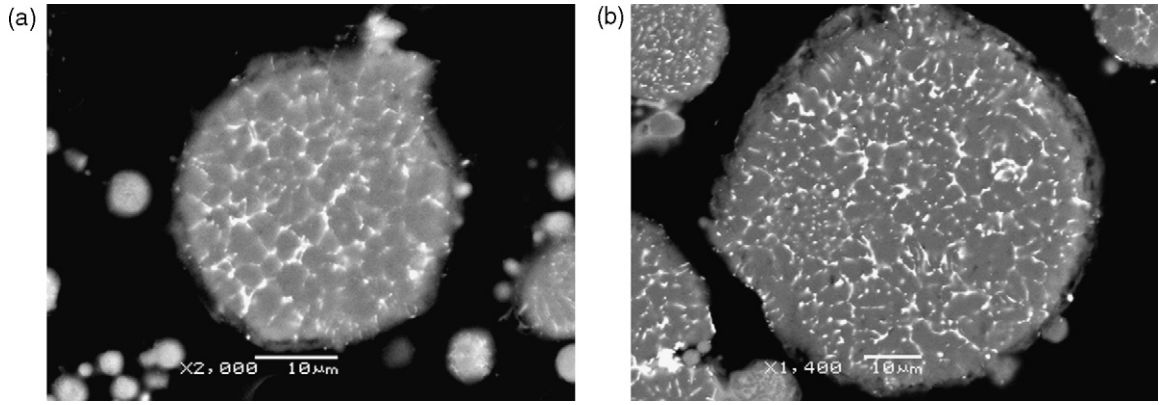

Fig. 2. Back scattered electron (BSE) images of cross-sectional structure of Al–Sn particles; (a) Al–5Sn and (b) Al–10Sn.

including microhardness and bonding strength of Al–Sn coating were investigated.

2. Experimental procedures

2.1. Materials and materials characterization

The gas atomized Al–Sn binary alloy powder containing 5 wt.% Sn and 10 wt.% Sn were used to prepare the Al–Sn coatings. Both feedstock powders present near-spherical morphologies, as shown in Fig. 1.

The cross-sectional microstructures of Al–5Sn and Al–10Sn feedstock powders are shown in Fig. 2. It is clear that the typical Al–Sn powders present the cellular or dendritic structure which results from the gas-atomized process of powder manufacturing. Tin phase (bright part) in backscattered electron (BSE) image presents a net-shape distribution in aluminum matrix (darker part).

The powder was sieved by #400 and #500 mesh with size of 26 and 38 μm, respectively. The size distribution of Al–5Sn and Al–10Sn powders by laser diffraction analysis is shown in Fig. 3. Al–5Sn and Al–10Sn powders present volume mean diameters (VMD) of 20.2 and 15.2 μm, respectively. Chemical analysis of composition reveals that the fraction of tin is 5.5 and 9.9 wt.% for Al–5Sn and Al–10Sn feedstock powder, respectively.

Grit blasted mild steel plate with a thickness of 4 mm was used as the substrate to prepare the Al–5Sn and Al–10Sn coatings with low pressure cold spray system. Al6061 plate without blasting was used as substrate for Al–5Sn with high pressure cold spray system.

The microstructures of coatings were investigated by OM (AX70TRF, OLYMPUS OPTICAL, Japan) and SEM (JSM6360LV, JEOL, Japan). Microhardness of the coatings was measured on cross-sectional surface by Vickers hardness tester (FV-700, Future-Tech., Japan) under the load of 500 gm and the holding time of 10 s. For each sample, 10–15 points in the cross-sectional surface of coating were tested to get the average value of microhardness.

2.2. Spray systems and conditions

A commercial low pressure cold spray system (DYMET 404) was used in the present study to prepare Al–5Sn and Al–10Sn coatings. In this system, propellant gas of nitrogen or helium with pressure of 0.7 MPa was preheated to about 300 °C and expanded with a de Laval nozzle to get a supersonic gas jet. Powder was injected into the

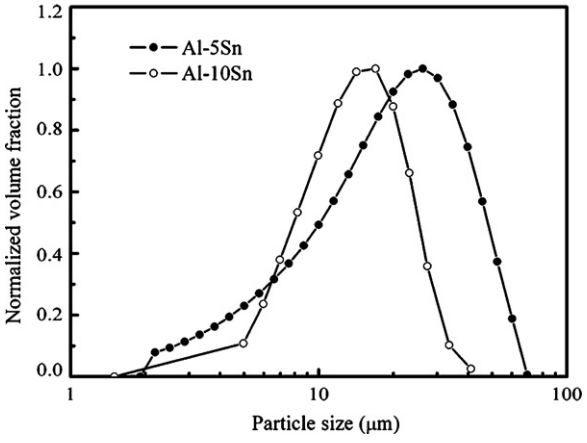

Fig. 3. Size distribution of Al–Sn feedstock powders.

supersonic jet from radial direction behind the throat of the nozzle by Venturi effect. The spray distance and traverse speed were fixed in 10 mm and 30 mm/s for the coating preparations in this study. The details of the system were described elsewhere [15].

The high pressure cold spray system developed in RIST was used to deposit Al–5Sn coatings. The system includes a powder carrier gas pre-heater as well as a main gas pre-heater. Nitrogen with a chamber pressure of 3 MPa and temperature of 500 °C was used as the propellant gas. Al–Sn powder was injected axially into the chamber of nozzle by carrier gas with pressure of 3.2 MPa which was preheated to a temperature of 300 °C by a separate resistant heater. The substrate moved with traverse speed of 40 mm/s and spray distance of 40 mm was utilized. The demonstrations of principle and setting of high pressure systems can be found in literatures [16].

2.3. Conditions of heat treatment and bond strength test

The as-sprayed coatings of Al–5Sn and Al–10Sn were annealed inside electrical resistant furnace to 150, 200, 250 and 300 °C and held for 1 h, respectively. Heating rate was set to 5 °C/min during all the heat treatments of coating samples. To avoid the serious oxidation of the coatings, nitrogen was used as the protecting gas during annealing. After heat-treated, the coatings were cooled to temperature of 50 °C inside the furnace and air cooled to room temperature.

Bond strength test was performed using a standard tensile strength test method according to ASTM standard C633-79. Al–Sn coating with a thickness of about 400–500 μm was deposited on the top of a grit blasted carbon steel stud with a diameter of 25.4 mm. As-sprayed and annealed samples were bonded to a blasted couple stud with adhesive agent (3 M DP-460) and cured at 50 °C for 3 h. The tensile strength test was performed under a displacement rate of 1 mm/min. Three to four samples for each condition were tested to get the average bond strength value in this study.

3. Results and discussions

3.1. Characteristics of the Al–Sn coatings

Fig. 4 shows the optical microstructures of as-sprayed coatings of Al–5Sn and Al–10Sn coatings on cross-sectional direction. It can be seen clearly that both Al–Sn coatings have quite dense structure with some pinholes in the coatings. For Al–5Sn coating on Al6061 substrate (Fig. 4(a)), the interface between coating and substrate (marked as black arrows in the photo) is almost undistinguishable in the OM photos. For Al–10Sn coating on mild steel substrate (Fig. 4(b)), the black line on the interface between coating and substrate is resulted from polishing process because of the different hardness of the coating and the substrate materials. All the structures of coatings suggested the good bonding between the coating and substrate.

The BSE image of the as-sprayed Al–5Sn and Al–10Sn coatings are shown in Fig. 5. In both Al–Sn coatings prepared with low pressure and high pressure cold spraying, the intensive deforma-

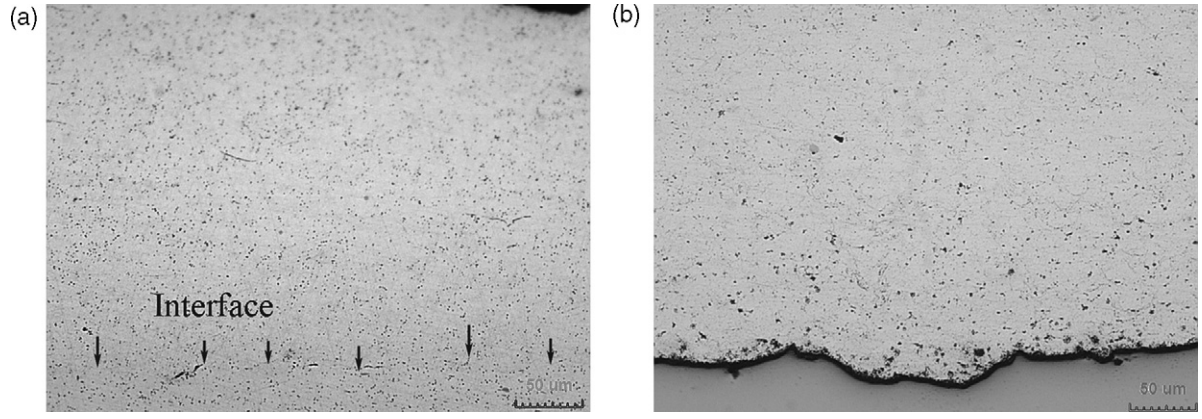

Fig. 4. Cross-sectional structure (OM) of Al–5Sn and Al–10Sn coatings near the coating-substrate interface; (a) Al–5Sn coating on Al6061 and (b) Al–10Sn coating on mild steel.

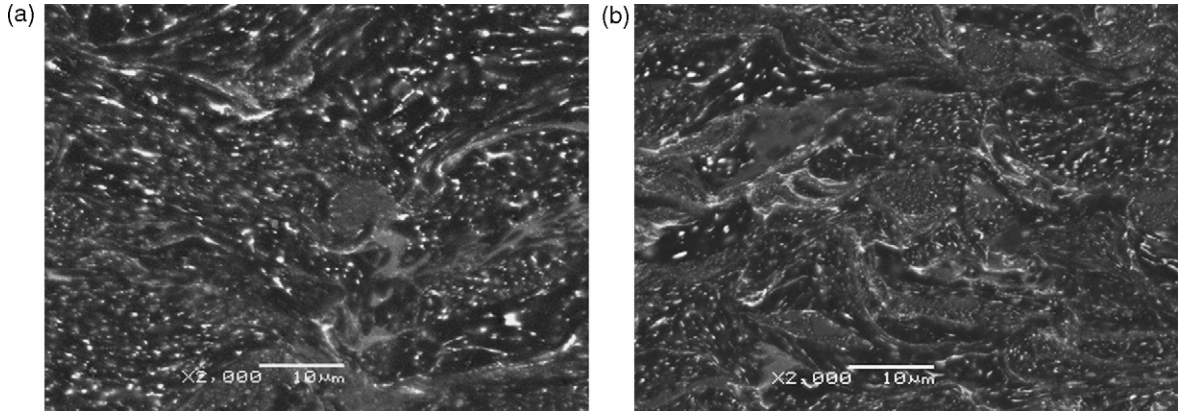

Fig. 5. Back scattered electron (BSE) microstructure of as-sprayed Al–Sn coatings; (a) Al–5Sn and (b) Al–10Sn.

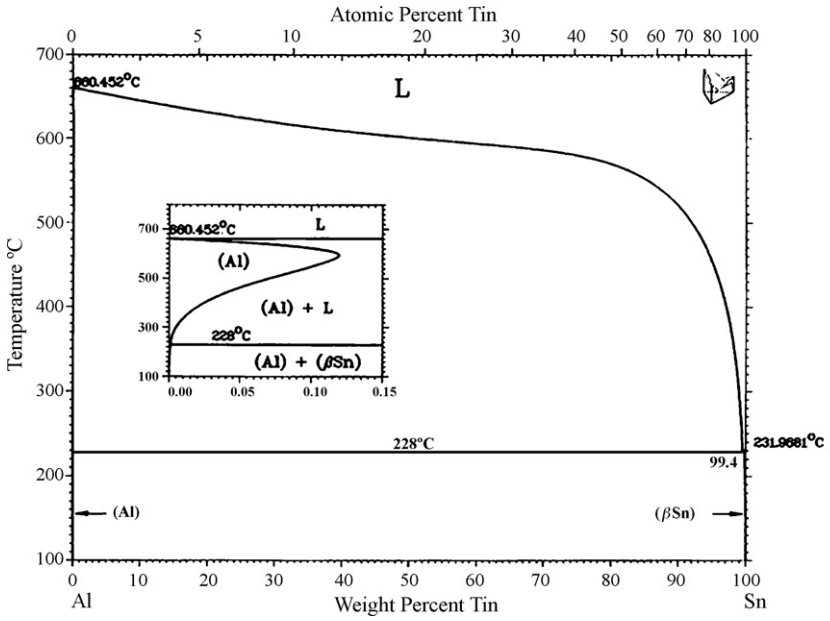

Fig. 6. Equilibrium phase diagram of Al–Sn binary alloy.

tion of the particle can be observed. Due to the smaller size of feedstock powders and using of He as the propellant gas, it can be suggested that the Al–10Sn particles can perform more effective accelerations during the low pressure cold spraying in this study. This resulted in the more intensive deformation on the outer region of particles during impact on substrate or pre-deposited particles, as can be found in Fig. 5(b).

The equilibrium phase diagram of Al–Sn binary alloy is shown in Fig. 6. The solubility of tin in aluminum at room temperature can be lower than 0.09–0.15 wt.% [16,17]. This can be confirmed from the microstructure of Al–Sn powders, i.e. tin distributed mainly in the aluminum matrix as a second phase (Fig. 2).

The experimental and modeling investigation of particle impact process by many researchers suggested that the bonding mechanism of particles in cold spray process involves the intensive localized deformation between particle–particle or particle–substrate interface, which can break the oxide layer of the particle or substrate surface and provide a close contact for fresh metal to make bonding. Typically, this peculiarity of cold spray process can result in the highly elongation of grains near the locally shear deformation region [18]. The intensive elongation of aluminum matrix near the interface of deformed particles was also observed in Al–Sn coatings which resulted in a near-lamellar structure of coatings.

Fig. 7 shows a typical deformed region near the particle boundary of Al–5Sn coating. The elongation of aluminum matrix resulted in the fragmentation of net-shape Sn in the deformed particles. EDXA analysis indicates that the fraction of tin in deformed region (marked as A) and aluminum matrix (marked as B) present the value of 0 and 5.7 wt.%, respectively. According to the literatures, the melting phenomenon was observed in cold spraying especially for the relatively low melting materials such as zinc, tin, etc. [19,20] However, theoretical analysis also indicates that the contact time during particle impact is of about 10^{-8} s. This makes the thermal diffusion distance during the particle impacting quite short [21]. On the other hand, the equilibrium solubility of tin in aluminum at room temperature is quite low, as shown before. Therefore, it can be supposed that the melting of tin and aluminum matrix did not play a role in forming this mixed region. It is believed that the intensive mixing of Al and Sn is mainly due to the plastic flow during particle impacting. In other word, this mixing phenomenon of Al and Sn can be considered as so called mechanical alloying effect. This structure can be comparable with the structure in thermal sprayed Al–Sn based alloy. Nevertheless, in thermal spray, this phenomenon was suggested from rapid cooling rate during the impacting of molten metal droplet [13,22].

3.2. Effect of heat treatment on Al–Sn coating microstructure

The BSE images of Al–5Sn and Al–10Sn coatings after heat treatment are shown in Figs. 8 and 9. Comparing with as-sprayed coating (Fig. 5(a)), no significant change of the microstructure of coating was observed after annealed at 150 °C. When heated at 250 and 300 °C, the coarsening and spheroidizing of Sn phase was observed in the Al–5Sn coating.

When the annealing temperature exceeds 230 °C, the melting of tin occurred. Therefore, the diffusion of the fragments of tin inside the deformed particles may result in the coarsening and migration of Sn. On the other hand, in the intensively mixed region of Sn and Al due to the shear strain, the re-precipitation and migration of tin can be supposed. All these Sn phase migrate to the particle

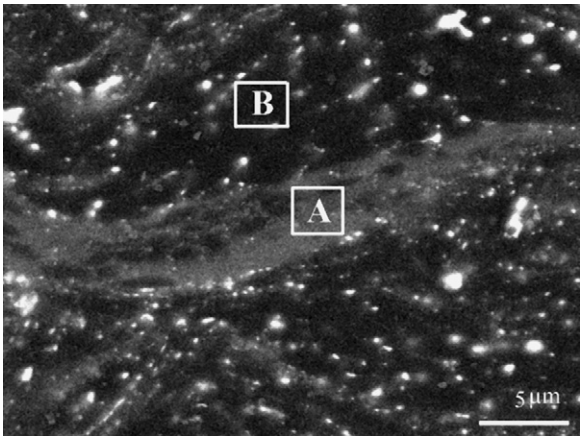

Fig. 7. Typical deformed particles in Al–5Sn coating.

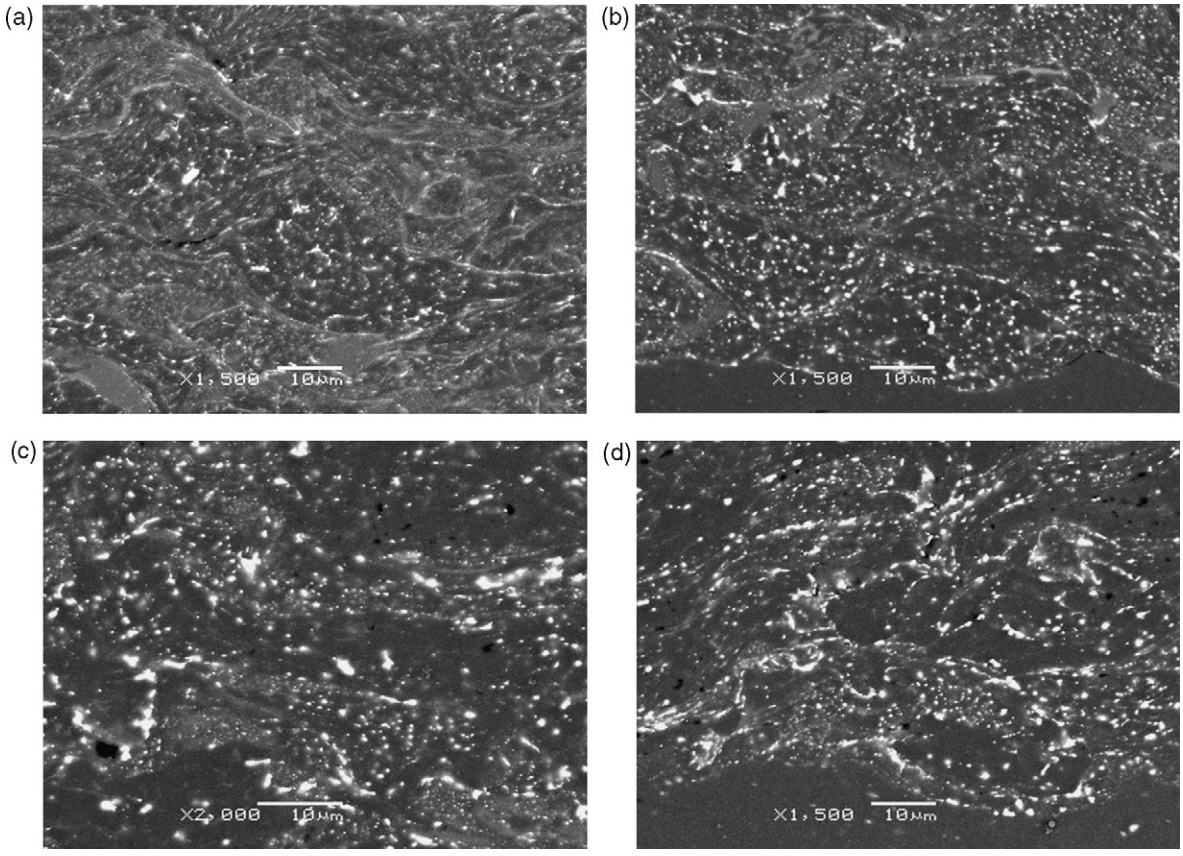

Fig. 8. Microstructures of annealed Al–5Sn coatings; (a) 150 °C, (b) 200 °C, (c) 250 °C and (d) 300 °C.

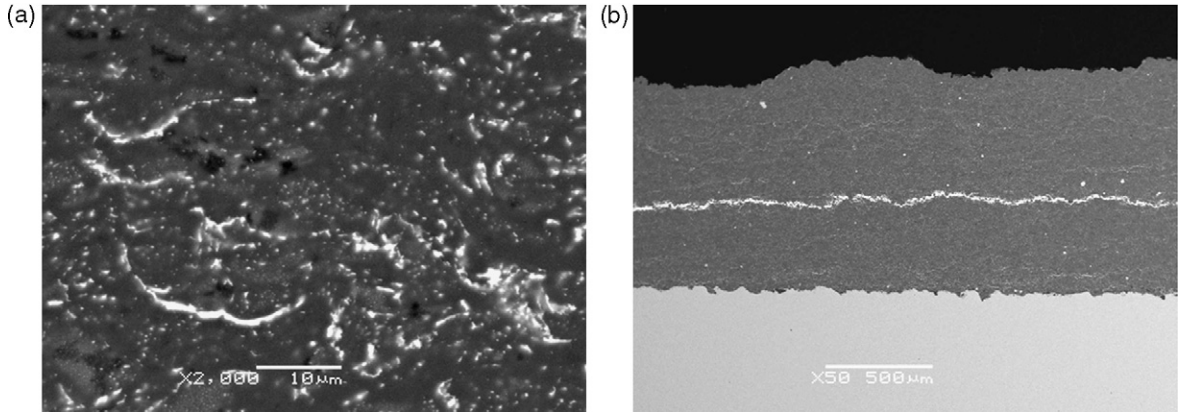

Fig. 9. Back scattered electron (BSE) microstructure of Al–10Sn coatings after heat treatment at 250 °C; note the sub-layer of Sn in the coating.

boundary during the annealing. Similar microstructure of Al–10Sn as Al–5Sn coating can be obtained after annealing at the temperature over the melting point of tin, as shown in Fig. 9(b). However, it should be noted that when Al–10Sn coating was annealed at 250 °C, the congregation of tin resulted in a sub-layer inside the coating and can result in the crack during the heat-treatment.

It is interesting to note in this study that even annealed at 200 °C, which is lower than the melting point of tin, the coarsening of Sn phase in both coatings can be observed. It can be supposed that this phenomenon is mainly based on the diffusion of tin under the solid state. Since the annealing temperature can exceed the melting point of tin in this study, the average content of Al–5Sn coatings after heat treatment were also investigated by EDXA. These results suggest that the fraction of tin in the heat treated coatings is consistent with that of as-sprayed coatings.

3.3. Effect of heat treatment on microhardness and bonding strength of Al–Sn coatings

Fig. 10 shows the effect of the annealing on microhardness of Al–Sn coatings as a function of the annealing temperature. The as-sprayed coatings of Al–5Sn and Al–10Sn present Vickers hardness (Hv 0.5) range from 71 to 76 and 72 to 75, which provide average value of 73 and 74, respectively. This value is much lower than the microhardness of 120 (Hv 0.3) for HVOF-sprayed Al20Sn1Cu2Ni coating and 150 (Hv 0.3) for Al–20Sn1Cu7Si coating reported in literature [18]. Microhardness of both coatings decreases at 200 °C

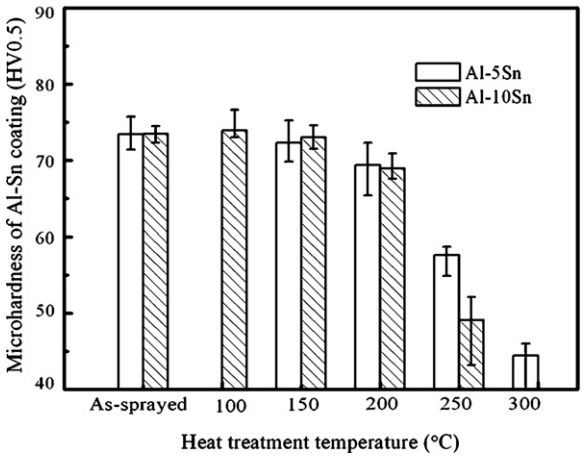

Fig. 10. Effect of heat treatment on the microhardness of Al–Sn coatings.

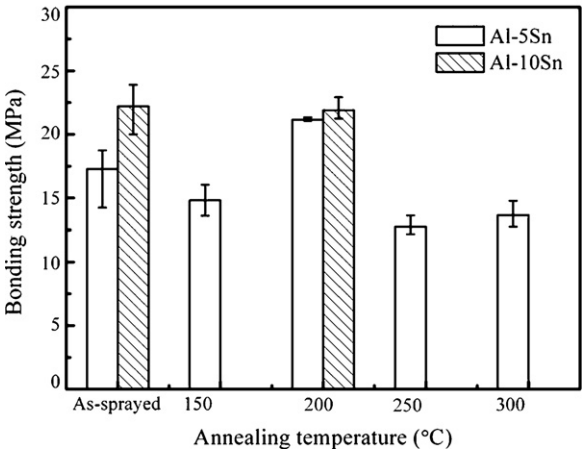

Fig. 11. Bond strength of as-sprayed and annealed Al–Sn coatings.

and significant decrease can be observed above 250 °C. Furthermore, the microhardness of Al–10Sn decreased more than that of Al–5Sn. The decrease of microhardness of annealed coatings may be caused by the residual stress relief of the Al matrix and the coarsening of Sn phase in the coatings.

Fig. 11 shows the bond strength of as-sprayed and annealed Al–Sn coatings. The as-sprayed Al–5Sn and Al–10Sn coatings present average bond strength of 17 and 22 MPa, respectively. This value is comparable to the bond strength of Al–Sn–Pb layer prepared by liquid–solid rolling process on the steel back, which ranged from 5 to 33 MPa [23]. However, compared with the reported bond strength of 55–75 MPa for cold-sprayed aluminum coating on Al6061 substrates, the bond strength of Al–Sn coatings is relatively low [24].

Notice that on the surface of feedstock powder (Fig. 12(a)), tin appear a net-shape distribution in the aluminum matrix. During the deposition of coatings, the melting of tin was observed due to the impacting of particle, as shown in Fig. 12(b). It was suggested that the existence of tin and the melting phenomenon of tin during particle impacting can increase the critical velocity of Al–Sn powder comparing with pure aluminum powder [14]. It implies that for the particle bonding, the existence of tin can also affect the bonding properties between particle and substrate.

It should be noted that all the failure during bonding test occurred on the interface of coating and substrate. This indicates that the interfacial property during coating preparation and heat treatment play a role in adhesion of coating. Xu et al. [23] pointed out that for the Al–Sn–Pb layer on the steel back prepared by liquid–solid rolling method, the bonding strength of Al–Sn–Pb layer depends significantly on the diffusion formed $FeAl_3$ layer during the wetting of aluminum on steel under high temperature. In the present study, no obvious diffusion was observed on the coating-substrate interface for as-sprayed and annealed coatings, which is consistent with HVOF-sprayed Al–Sn coatings [12,13]. As shown in Fig. 13, the EDS mapping of aluminum on the failed surface of substrate indicates clearly that more Al–Sn particles were bonded to the substrate as the annealing temperature exceed the melting point of tin. Naturally, one can expect the potential of enhanced bonding of the coating and substrate. However, the bonding strength of annealed samples of Al–5Sn decreased as the annealing temperature exceeds 250 °C.

According to the research of reaction between melted Sn and Fe, $FeSn_2$ and FeSn phase can be formed over melting point of tin and this phase can be detrimental to the bonding property of Sn–Ag solder to FeNi alloy [25]. In this study, the color of the substrate surface prove an obvious change after annealed at 250 and 300 °C comparing with as-sprayed and 200 °C annealed samples. This may be resulted from the reaction of Fe and Sn as the annealing temperature exceeds the melting point of tin. Therefore, the decrease of bonding strength during heat treatment above the melting point of Sn can be attributed to the formation of $FeSn_2$ and/or FeSn phase. Unfortunately, due to the fact that the tin phase on the substrate is quite small, it is quite difficult to detect the Fe–Sn phase effectively in this study.

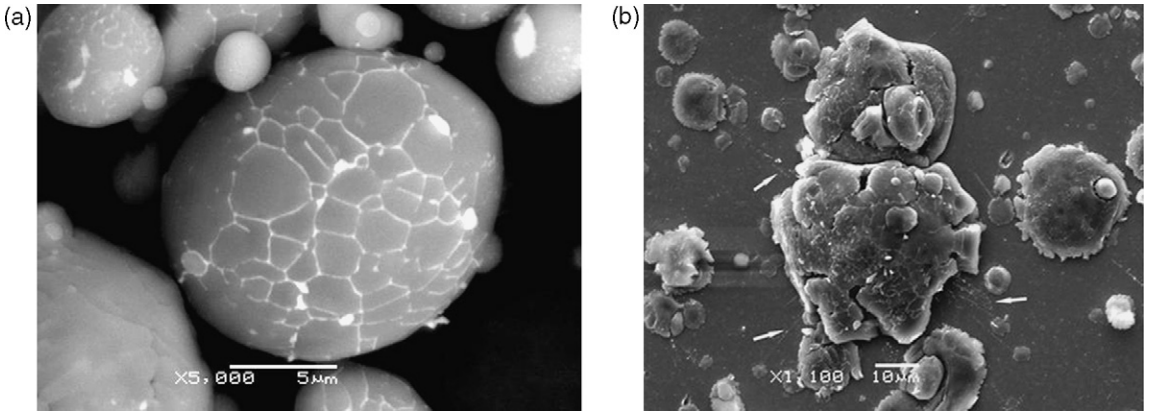

Fig. 12. The surface of feedstock powder (a) and bonded particle of Al–Sn on the substrate (b) (the melted tin was marked as white arrows in (b)).

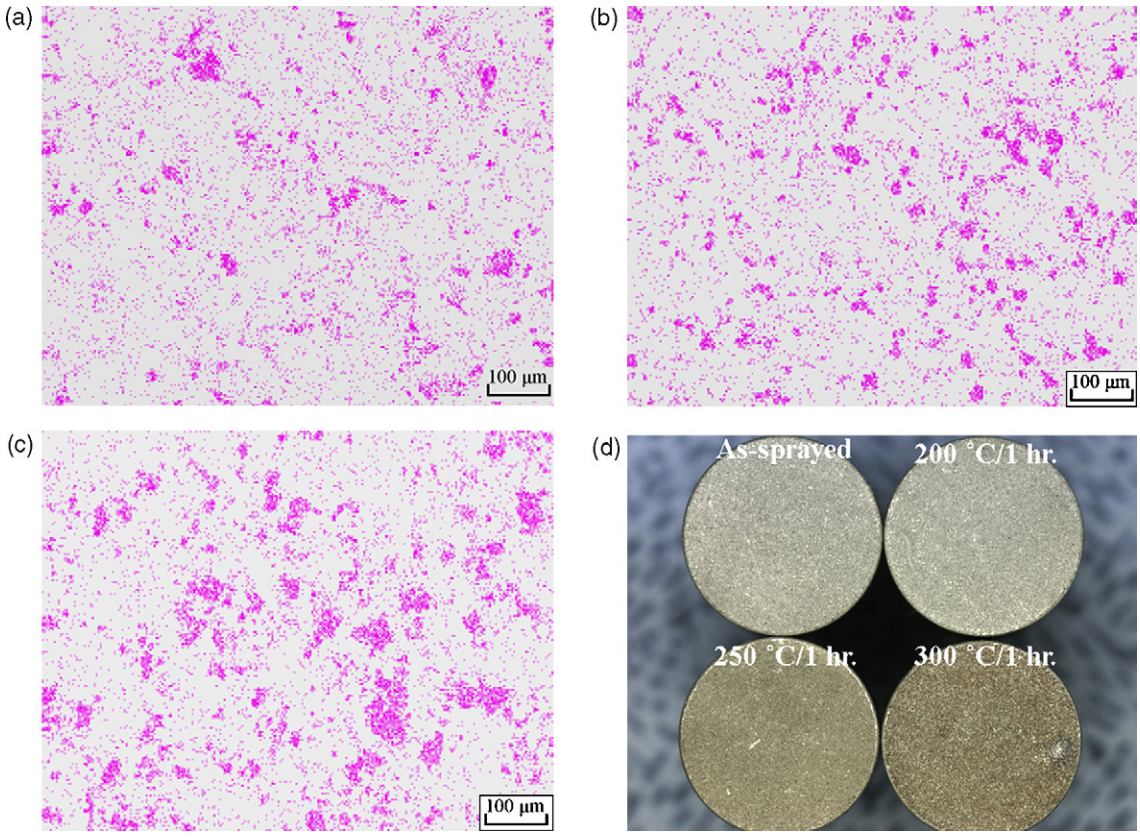

Fig. 13. EDXA mapping of aluminum element on substrate surface after annealed at (a) 200 °C, (b) 250 °C, (c) 300 °C and (d) macro pictures of substrate surface.

4. Conclusions

Al–Sn binary coatings can be successfully deposited by cold spray process. Both the Al–5Sn and Al–10Sn coatings present low porosity and well-bonded structures. The composition of Al–Sn coatings is consistent with that of feedstock powders. The as-sprayed Al–5Sn and Al–10Sn coatings present average value of hardness of about 73 and 74. The fraction of Sn phase in the as-sprayed Al–Sn coating is consistent with the feedstock powder.

Heat treatment at the temperature above the melting point of tin make the coarsening and spheroidizing of tin in the coating and decrease the microhardness significantly. During the heat treatment, the fraction of tin in the coating is consistent with the as-sprayed coatings and feedstock powders. The bond strength of as-sprayed coating presents a value of about 17 and 22 MPa for Al–5Sn and Al–10Sn which is comparable to that of liquid–solid rolling bonded Al–Sn–Pb layer on steel while is relatively lower than that of the cold-sprayed aluminum coatings on Al6061 substrate. The bond strength can be increased for Al–5Sn coating after annealed at 200 °C. However, bond strength of both coatings is again decreased when heat treated above the melting point of Sn, which may be resulted from the reaction of Fe and melted Sn and subsequently the formation of detrimental FeSn and/or $FeSn_2$ phase on the interface between coating and steel substrate.

Acknowledgements

This research was supported by a grant from the Center for Advanced Materials Processing (CAMP) of the 21st Century Frontier R&D Program funded by the Ministry of Commerce, Industry and Energy (MOCIE), Republic of Korea.

References

[1] A.P. Alkimov, A.N. Papyrin, V.F. Kosarev, N.I. Nesterovich, M.M. Shushpanov, U.S. Patent 5 302 414, April 12 (1994).
[2] V.F. Kosarev, S.V. Klinkov, A.P. Alkhimov, A.N. Papyrin, J. Therm. Spray Technol. 12 (2) (2003) 265.
[3] H. Assadi, F. Gärtner, T. Stoltenhoff, H. Kreye, Acta Mater. 51 (15) (2003) 4379.
[4] J. Vicek, L. Gimeno, H. Huber, E. Lugscheider, J. Therm. Spray Technol. 14 (1) (2005) 125.
[5] T. Stoltenhoff, H. Kreye, H.J. Richter, J. Therm. Spray Technol. 11 (2002) 542.
[6] S.V. Klinkov, V.F. Kosarev, M. Rein, Aerospace Sci. Technol. 9 (2005) 582.
[7] W.-Y. Li, H.-L. Liao, C.-J. Li, G. Li, C. Coddet, X.-F. Wang, Appl. Surf. Sci. 253 (2006 2852).
[8] S. Marx, A. Paul, A. Këhler, G. Hüttl, in: Proceedings of the ITSC2005, Basel, Switzerland, May 2–4, 2005, p. 209.
[9] F. Gärtner, T. Stoltenhoff, T. Schmidt, H. Kreye, in: Proceedings of the ITSC2005, Basel, Switzerland, May 2–4, 2005, p. 158.
[10] T. Desaki, Y. Goto, S. Kamiya, JSAE Rev. 21 (2000) 321.
[11] K. Lepper, M. James, J. Chashechkina, D.A. Rigney, Wear 203–204 (1997) 46.
[12] C. Perrin, S. Harris, D.G. McCartney, S. Syngellakis, P.A. Reed, in: J.F. Morton, B.C. Muddle (Eds.), Mater. Forum 28 (2004) 1371.
[13] C.J. Kong, P.D. Brown, S.J. Harris, D.G. McCartney, Mater. Sci. Eng. A 403 (2005) 205.
[14] X.-J. Ning, J.-H. Jang, H.-J. Kim, C.-J. Li, C. Lee, Surf. Coat. Technol. 202 (2008) 1681.
[15] X.-J. Ning, J.-H. Jang, H.-J. Kim, Appl. Surf. Sci. 253 (2007) 7449.
[16] H.-J. Kim, C. Lee, S.-Y. Hwang, Surf. Coat. Technol. 191 (2005) 335.
[17] A. Perrone, A. Zocco, H. de Rosa, R. Zimmermann, M. Bersani, Mater. Sci. Eng. C 22 (2002) 465.
[18] T.H. Van Steenkiste, J.R. Smith, R.E. Teets, Surf. Coat. Technol. 154 (2002) 237.
[19] W.-Y. Li, C. Zhang, X.P. Guo, L. Dembinski, H. Liao, C. Coddet, C.-J. Li, in: Proceedings of the ITSC2007, Beijing, P.R. China, May 14–16, 2007, p. 60.
[20] C.-J. Li, W.-Y. Li, H. S Fukanuma, in: Proceedings of the ITSC2004, Osaka, Japan, May 10–12, 2004, p. 335.
[21] M. Grujicic, C.L. Zhao, W.S. DeRosset, D. Helfritch, Mater. Des. 25 (2004) 681.
[22] T. Marrocco, L.C. Driver, S.J. Harris, D.G. McCartney, J. Therm. Spray Technol. 15 (2006) 634.
[23] G.-M. Xu, B.-M. Li, J.-Z. Cui, J. Iron Steel Res. Int. 13–4 (2006) 40.
[24] V.K. Champagne, The cold spray materials deposition process: fundamentals and applications, in: Woodhead Publishing Ltd., England, 2007, p. 66.
[25] E. Saiz, C.-W. Hwang, K. Suganuma, A.P. Tomsia, Acta Mater. 51 (2003) 3185.